
Orthogonal expression of an artificial metalloenzyme for abiological catalysis

Evan W. Reynolds[†], Timothy D. Schwochert[†], Matthew W. McHenry, John W. Watters, and Eric M. Brustad^{*}

Department of Chemistry, University of North Carolina at Chapel Hill, 125 South Road, CB 3290,
Chapel Hill, NC 27599.

^{*}Corresponding author, email: brustad@unc.edu

[†]These authors contributed equally to this work.

Table of Contents

Experimental Procedures	3
I. General methods and materials	3
II. Organic synthesis and characterization	3
IIA. Porphyrin synthesis.....	3
IIB. Cyclopropanation product standard synthesis	4
III. Plasmids and cloning	5
IV. Protein expression	5
V. Protein purification	5
VI. HPLC analysis of purified proteins for heme content.....	5
VII. Absorbance spectra of enzymes and the carbon monoxide binding assay	5
VIII. Enzymatic cyclopropanation reactions.....	5
Supplementary Tables	7
Table S1. Amino acid mutations present in BM3h variants used in this study.....	7
Table S2. UV-Vis absorbance of purified BM3h cofactor-substituted variants.....	7
Table S3. Gradient used for HPLC analysis of purified proteins.....	7
Table S4. Activities and stereoselectivities of biocatalysts for the reaction of tert-butyl acrylate with ethyl diazoacetate.....	8
Table S5. Activities and stereoselectivities of biocatalysts for the reaction of 1-octene with ethyl diazoacetate.....	9
Supplementary Figures	10
Figure S1. UV-Vis absorbance data of BM3h variants with Ir(Me)-DPIX, Fe-DPIX and heme cofactors.....	10
Figure S2. HPLC analysis of Ir(Me)-DPIX content in protein preparations.....	11
Figure S3. Relative yields of BM3h T268A, WIVS-FM T268A and WIVS-FM* T268A variants with Ir(Me)-DPIX.....	12
Figure S4. GC chromatographs for cyclopropanation reaction products using ethyl diazoacetate and styrene.....	13
Figure S5. Absorbance shifts for WIVS-FM* bound and free IrDPIX Me are retained following an enzymatic reaction.....	14
Figure S6. GC chromatographs for cyclopropanation products using ethyl diazoacetate and tert-butyl acrylate.....	16
Figure S7. GC chromatographs for cyclopropanation products using ethyl diazoacetate and 1-octene.....	17
Figure S8. GC/MS chromatographs separating trans cyclopropanation products using ethyl diazoacetate and tert-butyl acrylate.....	18
Figure S9. GC chromatographs separating cis cyclopropanation products using ethyl diazoacetate and 1-octene.....	19
Figure S10. Calibration curves used to determine cyclopropane product concentrations.....	20
NMR data	21
References	25
Author Contributions	25

Experimental Procedures

I. General methods and materials

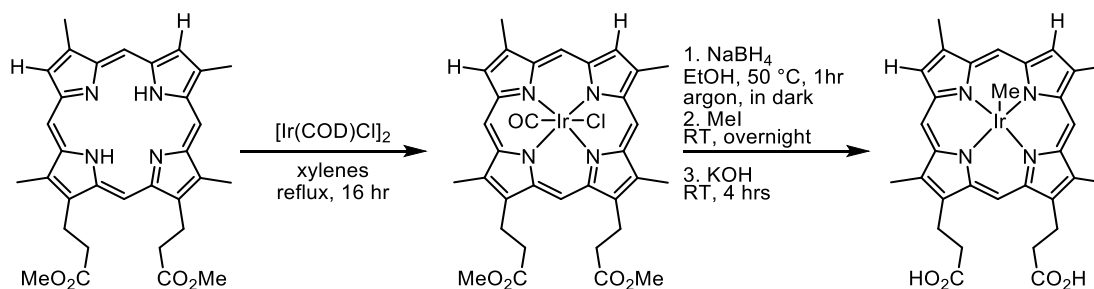
Deuteroporphyrin IX dimethyl ester was obtained from Frontier Scientific. Oligonucleotides were obtained from Integrated DNA Technologies. Enzymes and reagents used for cloning were obtained from New England BioLabs. All other chemical reagents and solvents were obtained from chemical suppliers (Acros, Fisher Scientific, or Sigma-Aldrich) and used without further purification.

Reactions requiring inert atmosphere were carried out in oven-dried glassware using standard Schlenk techniques under nitrogen. If required, solvents were degassed by bubbling with nitrogen. Reaction progress was monitored by thin layer chromatography (EMD Millipore TLC silica gel 60 F254). Silica gel chromatography was performed on an automated Biotage Isolera One using 50 g SNAP Ultra columns. Proton magnetic resonance spectra were acquired on 400 MHz Bruker instruments in the Department of Chemistry NMR facility at the University of North Carolina – Chapel Hill. NMR spectra were processed with ACD/NMR Processor (ACD/Labs). Chemical shifts are referenced to residual solvent peaks.^[1] Chiral GC analyses were obtained with Agilent 7820A gas chromatograph equipped with a FID detector and a J&W Scientific cyclosil-B column (30 m x 0.25 mm ID x 0.25 μm film) or a ThermoScientific Trace1310 equipped with an Exactive Orbitrap MS detector and an Astec Chiraldex B-DM column (30 m x 0.25 mm ID x 0.12 μm film). LC-MS analyses were obtained with an Agilent 6520 Accurate Mass QTOF LC-MS ESI positive in high-resolution mode, equipped with a Thermo Scientific Acclaim RSLC 120 C18 column (2.2 μm particle size, 120 Å pore diameter, 2.1 x 150 mm).

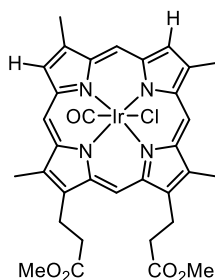
II. Organic synthesis and characterization

IIA. Porphyrin synthesis

General methods. The synthesis of Ir(Me)-DPIX was adapted from procedures for the synthesis of Ir(Me)-mesoporphyrin IX.^[2] The steps starting from commercial deuteroporphyrin IX dimethyl ester (Frontier Scientific) are described below (**Scheme S1**).



Scheme S1. Ir(Me) deuteroporphyrin IX synthesis.

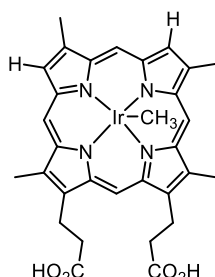


II.A.i. Ir(CO)Cl-deuteroporphyrin IX dimethyl ester

A solution of deuteroporphyrin IX dimethyl ester (95 mg, 0.18 mmol) and $[\text{Ir}(\text{COD})\text{Cl}]_2$ (155 mg, 0.23 mmol) in xylenes (100 mL) was refluxed under an air atmosphere. Reaction progress was monitored by TLC with 1:1 hexane to ethyl acetate as the mobile phase. The reaction typically went overnight to reach completion. The solvent was removed via rotary evaporation and purified by column chromatography on silica gel. Impurities were first eluted with a gradient from 0 – 25 % ethyl acetate in hexane, then product was eluted as a pink band with a gradient from 25 – 50 % ethyl acetate in hexane. After evaporating the solvent, the purified product was redissolved in approximately 10 mL DCM and diluted with 100 mL hexane. The mixture was concentrated under vacuum resulting in precipitation of the pure product which was isolated by filtration as a red solid yielding 75 mg (53% yield). ¹H NMR (CDCl₃, 400 MHz) δ 10.38 (d, J = 5.5 Hz, 2H), 10.32 (s, 1H), 10.27 (s, 1H), 9.21 (s, 1H), 9.18 (s, 1H), 4.51-4.46 (m, 4H), 3.83 (d, J = 9.7 Hz, 6H), 3.76-

3.66 (m, 12H), 3.39 (t, $J = 7.8$ Hz, 4H) ppm. ^{13}C NMR (CDCl_3 , 151 MHz) δ 173.70, 173.69, 141.59, 141.20, 139.93, 139.85, 139.76, 139.54, 139.49, 139.31, 139.23, 139.14, 139.09, 138.96, 137.91, 137.89, 134.58, 129.88, 129.77, 102.71, 101.91, 99.86, 98.60, 51.92, 51.91, 36.87, 21.91, 21.87, 14.08, 14.02, 11.91, 11.86 ppm. Calculated $[\text{M}+\text{Na}]^+ = 815.1592$ found $[\text{M}+\text{Na}]^+ = 815.1553$. UV-Vis (CH_2Cl_2 , concentration = 5×10^{-6} M) λ_{max} ($\epsilon \text{ mM}^{-1}\text{cm}^{-1}$) 400 (95.6), 514 (14.8), 546 nm (23.5).

II.A.ii. Ir(Me)-deuterioporphyrin IX

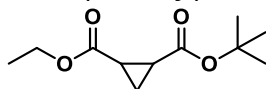


To a solution of Ir(CO)Cl-deuterioporphyrin IX dimethyl ester (70 mg, 0.088 mmol) in degassed, anhydrous ethanol (10 mL), a degassed solution of NaBH_4 (17 mg, 0.44 mmol) and NaOH (1 M) in water (3 mL) was added under nitrogen atmosphere. A color change from bright red to dark red-brown was observed upon addition of NaBH_4 to the porphyrin solution. The mixture was stirred for 1 hour at 50°C in the dark. Following this, the reaction was cooled to room temperature and methyl iodide (6 mL) was added. The reaction was then stirred overnight at room temperature under an argon atmosphere. The reaction mixture was concentrated to ~ 2 mL by rotary evaporation, and potassium hydroxide (300 mg) was added to achieve hydrolysis of the methyl esters. The reaction was stirred at room temperature under argon and progress was monitored by TLC using 3% MeOH in DCM as the mobile phase. Upon completion (~ 4 hrs), the reaction was diluted in sodium phosphate buffer (10 mL, 0.1 M, pH 5) and acidified with HCl (1 M) to pH ~ 5 . The resulting red precipitant was collected via centrifugation ($4000 \times g$, 15 min, 4°C) and the supernatant discarded. The solid was resuspended in water (15 mL) and centrifuged again. The resulting solid was dried under high vacuum overnight to yield the product as a dark red powder 49 mg (78% yield). ^1H NMR (CD_3CN , 400 MHz) δ 9.88-9.78 (m, 4H), 8.84 (d, $J = 9.4$ Hz, 2H), 4.31-4.27 (m, 4H), 3.71 (s, 3H), 3.68 (s, 3H), 3.62 (s, 3H), 3.57 (s, 3H), 3.28-3.24 (m, 4H), -7.94 (s, 3H) ppm. ^{13}C NMR (176 MHz, $\text{DMSO}-d_6$) δ 174.71, 174.69, 141.18, 140.99, 140.88, 140.74, 140.69, 140.49, 140.46, 140.42, 140.38, 140.18, 139.55, 139.41, 137.07, 136.93, 129.86, 129.70, 103.26, 102.34, 100.09, 99.21, 40.53, 40.39, 40.27, 40.15, 40.03, 39.91, 39.79, 39.68, 37.71, 21.82, 13.96, 13.90, 11.75, 11.71, -26.57. Calculated $[\text{M}+\text{H}]^+ = 717.2048$ found $[\text{M}+\text{H}]^+ = 717.2007$. UV-Vis (CH_3OH , 3.8×10^{-6}) λ_{max} ($\epsilon \text{ mM}^{-1}\text{cm}^{-1}$) 387 (121.1), 498 (8.5), 526 nm (13.3).

IIB. Cyclopropanation product standard synthesis

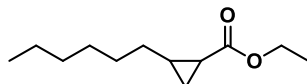
General methods. Cyclopropane product yields for ethyl 2-phenylcyclopropane-1-carboxylate were determined by generating a calibration curve (Fig. S5C) from product standard prepared as described previously.^[3] Cyclopropanation product standards for tert-butyl acrylate and 1-octene were synthesized using 5,10,15,20-Tetraphenyl-21H,23H-porphine iron(III) chloride as a catalyst. First, 0.0335g (0.0476mmol) of 5,10,15,20-tetraphenyl-21H,23H-porphine iron(III) chloride, 0.264g and a reducing agent, iron(II) sulfate heptahydrate, were added to a round bottom flask and degassed with nitrogen. To this flask 5mL of dichloromethane was added and the solution was sparged with nitrogen. 0.95 mmol of olefin (1-octene or tert-butyl acrylate) was then added to the flask followed by slow addition of 100 μL (0.95 mmol) of ethyl diazoacetate via syringe pump over 4 hours. The reaction mixture was stirred for 12 hours under nitrogen atmosphere. The mixture was filtered through celite and the solvent was evaporated off using air. The resulting mixture was then purified on silica gel using n-pentane and diethyl ether as the mobile phase. The excess pentane and diethyl ether were removed using air.

IIB.i. 1-(tert-butyl) 2-ethyl cyclopropane-1,2-dicarboxylate



The product was synthesized following the general cyclopropanation method with tert-butyl acrylate as the olefin. The enantiomer mixture of the trans diastereomer products was isolated on silica gel as a clear oil using 95:5 pentane:diethyl ether as the mobile phase. The experimental spectra match previously reported characterization for the trans diastereomer.^[4] The CIS diastereomer was obtained as a crude mixture and was used to determine product elution times on GC. ^1H NMR (400 MHz, Chloroform- d) δ 4.20 – 4.14 (m, 2H), 2.16 – 2.05 (m, 2H), 1.47 (s, 9H), 1.39 (t, 2H), 1.30 (t, $J = 7.1, 1.9$ Hz, 3H). ^{13}C NMR (151 MHz, Chloroform- d) δ 172.2, 170.9, 81.28, 61.05, 28.05, 23.47, 22.13, 15.30, 14.20.

IIB.ii. ethyl 2-hexylcyclopropane-1-carboxylate



The product was synthesized following the general cyclopropanation protocol with 1-octene as the olefin. The enantiomer mixture of trans diastereomer products was isolated on silica gel as a clear oil using 99:1 pentane: diethyl ether as the mobile phase. The experimental spectra match previously reported characterization for the trans diastereomer.^[5] The CIS diastereomer was obtained as a crude mixture and was used to determine product elution times on GC. ¹H NMR (600 MHz, Chloroform-*d*) δ 4.13 (q, *J* = 7.1 Hz, 2H), 1.45 – 1.22 (m, 13H), 1.16 (dt, *J* = 8.7, 4.5 Hz, 1H), 0.90 (t, *J* = 7.0 Hz, 3H), 0.70 (ddd, *J* = 8.0, 6.3, 4.0 Hz, 1H). ¹³C NMR (151 MHz, Chloroform-*d*) δ 174.8, 60.34, 33.07, 31.81, 29.03, 28.99, 23.03, 22.65, 20.23, 15.59, 14.21, 14.12.

III. Plasmids and cloning

BM3 variants and the heme transport protein, ChuA, were cloned in the plasmids pCWori and pChuA, respectively, as described elsewhere^[6,7]. Site-specific mutants were assembled via scarless restriction ligation of BsaI digested PCR fragments containing the desired mutation. Primer sequences are available upon request. See **Table S1** for a list of amino acid mutations in the BM3 variants used in this study.

IV. Protein expression

Native heme-BM3 variants were expressed as previously described.^[3] Expression of BM3 variants containing Ir(Me)-DPIX was accomplished by slight modification of a previously described methodology.^[8] BM3h variants in pCWori were co-transformed with pChuA into electrocompetent *E. coli* BL21-AI cells (Novagen). For expressions in minimal media, individual colonies were inoculated into liquid starter cultures of M9 minimal media supplemented with 0.5 % glucose, 0.2 % cas amino acids, 340 μ g/mL thiamine hydrochloride, 2 mM MgSO₄, 0.1 mM CaCl₂, 100 μ g/mL kanamycin and 200 μ g/mL ampicillin. For rich media expressions, colonies were inoculated into liquid starter cultures of LB media supplemented with 100 μ g/mL kanamycin and 200 μ g/mL ampicillin. The cultures were grown overnight at 37 °C and 225 rpm. One liter of M9 minimal media or TB supplemented with 100 μ g/mL kanamycin and 200 μ g/mL ampicillin was inoculated with 5 mL of overnight starter culture (the M9 or LB culture, respectively) and incubated for 3-4 hours at 37 °C and 225 rpm to an OD_{600nm} of 0.6-0.7. The cultures were then induced by adding arabinose (to induce ChuA expression in BL21-AI) and Isopropyl β -D-thiogalactopyranoside (IPTG) to a final concentration of 0.2 % w/v and 1 mM, respectively. Due to observed decomposition of Ir(Me)-DPIX solutions when exposed to light, concentrated stock solutions of Ir(Me)-DPIX were freshly prepared at the time of induction by dissolving the solid in DMSO and diluting 10-fold in 0.1 M potassium phosphate, pH 12. The Ir(Me)-DPIX solution was added to the culture upon induction to a final concentration of 10 μ M. Upon induction, the incubation temperature was reduced to 25 °C and expressions were allowed to continue for 16-20 hours. After harvesting the cells by centrifugation (4 °C, 10 min, 4,000 \times g), the cell pellets were frozen at -20 °C for at least 2 hours.

V. Protein purification

Proteins were purified via 6 \times His-tag purification on a Ni-NTA HisTrap HP column (5 mL HisTrap HP, GE Healthcare, Piscataway, NJ) using an ATKA Purifier (GE Healthcare), as described elsewhere^[8]. Following purification, the protein was exchanged into 0.1 M potassium phosphate buffer, pH 8.0, with a 30 kDa molecular weight cut-off Amicon centrifugal filtration device (EMD Millipore), flash frozen on dry ice, and stored at -20 °C.

VI. HPLC analysis of purified proteins for heme content

The procedure for HPLC analysis of proteins was adapted from a method for analysis of Fe-DPIX enzymes.^[8] Proteins for HPLC analysis were exchanged into distilled water via dialysis or a 30 kDa molecular weight cut-off Amicon centrifugal filter (EMD Millipore). Proteins were diluted to approximately 5 μ M in distilled water and filtered through glass wool plugs prior to HPLC analysis on a 1260 Infinity binary liquid chromatography system (Agilent). Separations were achieved on a Restek Viva C4 column (5 μ m, 2.1 \times 150 mm) using the gradient described in **Table S3**. Calibration curves (**Figure S3**) were generated for Ir(Me)-DPIX and heme by monitoring absorbance at 395 nm to determine metalloporphyrin concentrations in the protein sample.

VII. Absorbance spectra of enzymes and the carbon monoxide binding assay

All absorbance measurements for protein samples were carried out in 0.1 M potassium phosphate buffer, pH 8. UV-vis data was obtained on a Tecan M1000 PRO UV/Vis plate reader or Cary 100 UV/Vis spectrometer (Agilent). The carbon monoxide difference spectra for native heme P450 enzymes were obtained as previously described in multiwell plate format.^[3] The absorbance spectrum of WIVS-FM*-T268A/C400G/Ir(Me)-DPIX was measured and compared with exact Ir(Me)-DPIX content determined via HPLC as described above. From these data, the extinction coefficient for the Soret peak was determined to be $\epsilon_{402nm} = 107.7 \text{ mM}^{-1}\text{cm}^{-1}$.

VIII. Enzymatic cyclopropanation reactions

Small scale (400 μ L) anaerobic reactions were setup in 2 mL crimp vials (Agilent). A solution of 0.1 M sodium phosphate buffer and 0.1M sodium chloride (pH 6.0) was degassed in a sealed vial for at least 10 minutes prior to use. For heme enzyme reactions, a sodium dithionite solution (100 mM in 0.1 M sodium phosphate buffer and 0.1M sodium chloride (pH 6.0)) was also degassed. The headspace of a sealed crimp vial containing enzyme in 0.1 M potassium phosphate buffer (pH 6.0) (or Ir(Me)-DPIX in 0.1 M NaOH) and a stir bar was flushed with argon, taking care to avoid bubbling of the protein solution. Using glass syringes, the buffer solution

was added under argon to a final volume of 380 μL . 10 μL of an olefin solution (4 M or 300 mM in DMF) was then added via syringe and allowed to mix for 30 seconds prior to adding 10 μL of ethyl diazoacetate (400 mM in DMF). The final concentrations of the reagents were: 16.67 or 20 μM catalyst, 7.5 or 100mM olefin, and 10 mM ethyl diazoacetate in 0.1 M sodium phosphate, 0.1M sodium chloride (pH 6.0) with 5% DMF. Heme enzyme reactions also included 10mM sodium dithionite. The vial was removed from the argon line, the septum covered with parafilm, and the reaction was allowed to stir overnight at room temperature. Reactions were quenched by the addition of 1 mL of ethyl acetate to precipitate the protein. Then, 20 μL of an internal standard solution (100 mM cyclopropyl phenyl ketone or prophiophenone in EtOH) was added. The mixture was transferred to a 1.7 mL microcentrifuge tube, vortexed, and centrifuged at 18,400 \times g for 2 minutes. The ethyl acetate layer was then dried with a small amount of sodium and filtered. The product mixtures were then analyzed on chiral GC. Separations on GC for reactions with styrene were achieved with at a constant pressure and a GC oven temperature gradient of 100 $^{\circ}\text{C}$ for 30 min, 1 $^{\circ}\text{C}/\text{min}$ to 135 $^{\circ}\text{C}$, 135 $^{\circ}\text{C}$ for 10 min, 10 $^{\circ}\text{C}/\text{min}$ to 200 $^{\circ}\text{C}$, and 200 $^{\circ}\text{C}$ for 5 min. Styrene cyclopropane product yields were determined by generating a calibration curve (Fig. S10C) from product standard prepared as described previously.³ Separations on GC for reactions with tert-butyl acrylate or 1-octene were achieved with pressure and an isocratic GC oven temperature of 90 $^{\circ}\text{C}$ for 35 mins, followed by a 10 $^{\circ}\text{C}/\text{min}$ ramp to 200 $^{\circ}\text{C}$ for 11 mins and 200 $^{\circ}\text{C}$ for 5 min (method A). Separation of the trans tert-butyl acrylate cyclopropanation products was achieved under constant pressure with a 90 $^{\circ}\text{C}$ isocratic method followed by a 10 $^{\circ}\text{C}/\text{min}$ ramp to 200 $^{\circ}\text{C}$ for 11 mins and 200 $^{\circ}\text{C}$ for 5 min using an Astec Chiraldex B-DM column (30 m \times 0.25 mm ID \times 0.12 μm film) on a ThermoScientific Trace1310 equipped with an Exactive Orbitrap MS detector. Separation of the cis octene cyclopropanation products was achieved with a constant pressure and an isocratic GC oven temperature of 90 $^{\circ}\text{C}$ for 80 mins followed by a 10 $^{\circ}\text{C}/\text{min}$ ramp to 200 $^{\circ}\text{C}$ for 11 mins and 200 $^{\circ}\text{C}$ for 5 min. Tert-butyl acrylate and 1-octene cyclopropane product yields were determined by generating a calibration curve (Fig. S10A and B) from synthesized product standards (IIB).

Supplementary Tables

Table S1. Amino acid mutations present in BM3h variants used in this study.

Variant	Amino Acid Sequence/Mutations relative to Parent
BM3h (Parent)	MTIKEMPQPKTFGELKNLPLLNTDKPVQALMKIADELGEIFKFEAPGRVTRY LSSQRLIKEACDESRFDKNSQALKFVRDFAGDGLFTSWTHEKNWKKAHN ILLPSFSQQAMKGYHAMMVDIAVQLVQKWERLNADEHIEVPEDMTRLTLDT IGLCGFNYRFNSFYRDQPHPFITSMVRALDEAMNKLQRANPDDPAYDENK RQFQEDIKVMNDLVDKIIADRKASGEQSDDLTHMLNGKDPETGEPLDDEN IRYQIITFLIAGHETTSGLLSFALYFLVKNPHVLQKAAEEAARVLVDPVPSYK QVKQLKYVGMVLNEALRLWPTAPAFSLYAKEDTVLGGEYPLEKGDLMVLI PQLHRDKTIWGDDVEEFRPERFENPSAIPQHAFKPFNGNGQRACIGQQFAL HEATLVLGMMMLKHDFEDHTNYELDIKETLTLKPEGFVVKAKSKKIPLGGIP SPSTLEHHHHHH
WIVS-FM	G265F, T269V, L272W, L322I, F405M, A406S
WIVS-FM*	WIVS-FM + L52I, I366V
WIVS-FM*-T268A	WIVS-FM* + T268A
WIVS-FM*-T268A/C400G	WIVS-FM* + T268A, C400G
WIVS-FM*-T268A/C400A	WIVS-FM* + T268A, C400A
WIVS-FM*-T268A/C400G/F87A	WIVS-FM* + F87A, T268A, C400G
WIVS-FM*-T268A/C400G/I263F	WIVS-FM* + I263F, T268A, C400G
WIVS-FM*-T268A/C400G/F87A/I263F	WIVS-FM* + F87A, I263F, T268A, C400G
WIVS-FM*-T268A/C400G/F87W	WIVS-FM* + F87W, T268A, C400G

Table S2. UV-Vis absorbance of purified BM3h cofactor-substituted variants.

Variant ^a	Condition	Soret band (nm)	Q bands (nm)
BM3h/heme	-	421	540, 576
	+ Na ₂ S ₂ O ₄	413	551 (broad)
	+ Na ₂ S ₂ O ₄ + CO	450	554 (broad)
WIVS-FM/Fe-DPIX	-	413	526, 552
	+ Na ₂ S ₂ O ₄	409	532(broad)
	+ Na ₂ S ₂ O ₄ + CO	430	535 (broad)
BM3h T268A/Ir(Me)-DPIX	-	402, 438	518, 546
BM3h T268A C400A/Ir(Me)-DPIX	-	402	508, 534
BM3h T268A C400G/Ir(Me)-DPIX	-	402	508, 534
WIVS-FM T268A/Ir(Me)-DPIX	-	406, 432	508, 534
WIVS-FM T268A C400A/Ir(Me)-DPIX	-	402	508, 534
WIVS-FM T268A C400G/Ir(Me)-DPIX	-	402	508, 534
WIVS-FM* T268A/Ir(Me)-DPIX	-	406, 432	508, 536
WIVS-FM* T268A C400A/Ir(Me)-DPIX	-	402	506, 534
WIVS-FM* T268A C400G/Ir(Me)-DPIX	-	402	506, 534

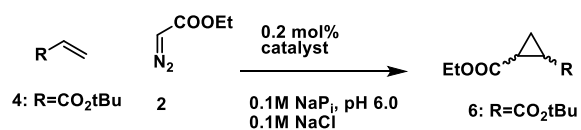
^aVariants with only one condition reported showed no change in the absorbance spectra upon addition of dithionite and exposure to CO.

Table S3. Gradient used for HPLC analysis of purified proteins.

Time (min)	% A (H ₂ O + 0.1% formic acid)	% B (MeCN + 0.1% formic acid)
0	50	50
10	20	80
10.01	5	95
17	5	95
17.01	50	50
20	50	50

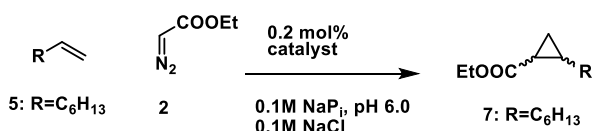
Separations were achieved on a Restek Viva C4 column (5 μm, 2.1 x 150 mm) with flow rate 0.4 mL/min

Table S4. Activities and stereoselectivities of biocatalysts for the reaction of tert-butyl acrylate with ethyl diazoacetate.



catalyst	yield (%)	TTN	dr (cis:trans)	ee _{trans} (%)	ee _{cis} (%)
heme	6	29	31:69	n.d.	n.d.
Ir(Me)-DPIX	8	40	16:84	<1	9.38
BM3h/heme	7	35	43:57	n.d.	n.d.
WIVSFM*-T268A/C400G/Ir(Me)-DPIX	29	147	13:87	2.9	13.9
WIVSFM*-T268A/F87A/C400G/Ir(Me)-DPIX	32	163	13:87	5.0	7.9
WIVSFM*-T268A/I263F/C400G/Ir(Me)-DPIX	26	131	16:84	13.4	1.6
WIVSFM*-T268A/F87A/I263F/C400G/Ir(Me)-DPIX	29	146	16:84	4.4	<1
WIVSFM*-T268A/F87W/C400G/Ir(Me)-DPIX	25	125	16:84	8.0	1.2

reaction conditions: 100 mM olefin, 10 mM EDA, 20 μ M catalyst, in 0.1 M NaPi, pH 6.0 100 mM NaCl buffer, 5% DMF as cosolvent (reactions with heme and heme enzymes also contain 10 mM dithionite). TTN and diastereoselectivities determined by chiral GC analysis. Enantiomers could not be resolved by chiral GC. TTN = total turnover number. Diastereomer identity determined by comparison to authentic standards. n.d. = not determined: low GC signal precluded accurate ee measurements.

Table S5. Activities and stereoselectivities of biocatalysts for the reaction of 1-octene with ethyl diazoacetate.

catalyst	yield (%)	TTN	dr (cis:trans)	ee _{cis} (%)
heme	n.d.	n.d	n.d	n.d
Ir(Me)-DPIX	5	23	30:70	<1
BM3h/heme	n.d.	n.d	n.d	n.d
WIVSFM*-T268A/C400G/Ir(Me)-DPIX	11	55	26:74	10.3
WIVSFM*-T268A/F87A/C400G/Ir(Me)-DPIX	17	83	27:31	11.4
WIVSFM*-T268A/I263F/C400G/Ir(Me)-DPIX	17	85	27:31	3.9
WIVSFM*-T268A/F87A/I263F/C400G/Ir(Me)-DPIX	18	92	29:71	4.3
WIVSFM*-T268A/F87W/C400G/Ir(Me)-DPIX	19	93	27:73	12.7

reaction conditions: 100 mM olefin, 10 mM EDA, 20 μ M catalyst, in 0.1 M NaPi pH 6.0 100 mM NaCl buffer, 5% DMF as cosolvent (reactions with heme and heme enzymes also contain 10 mM dithionite). TTN and diastereoselectivities determined by chiral GC analysis. *Trans* enantiomers could not be resolved by chiral GC. TTN = total turnover number. Diastereomer identity determined by comparison to authentic standards. n.d. = not detected.

Supplementary Figures

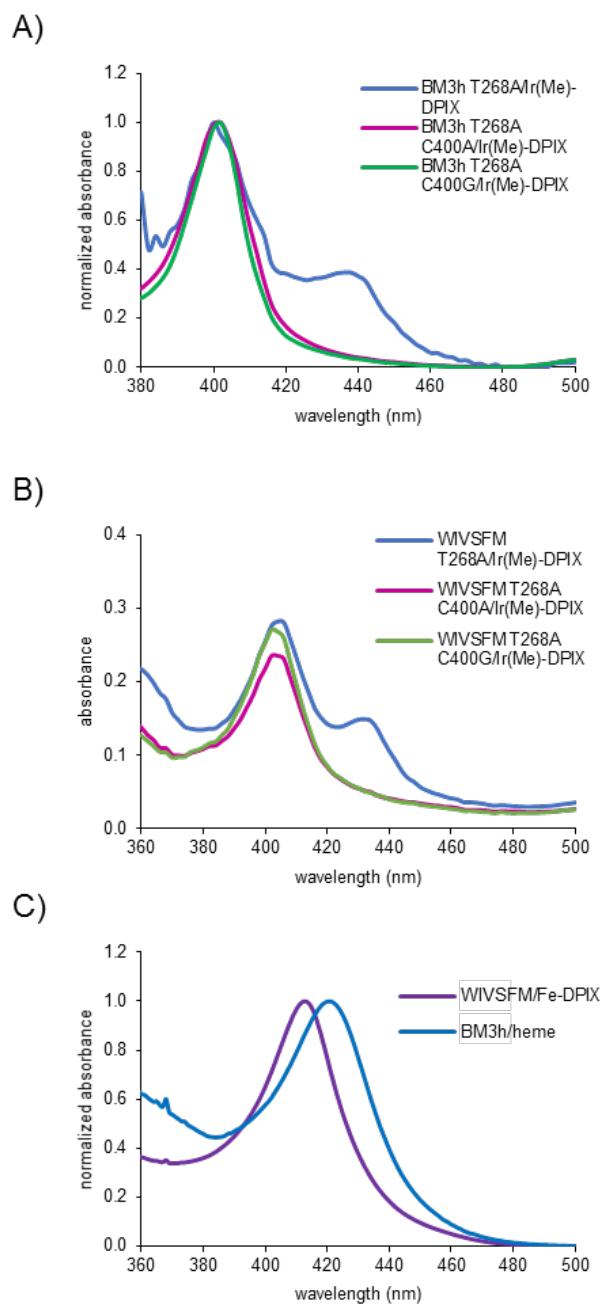


Figure S1. UV-Vis absorbance data of BM3h variants with Ir(Me)-DPIX, Fe-DPIX and heme cofactors. UV-Vis data is shown for the C400 (blue), C400A (violet) and C400G (green) variants of BM3h T268A (A) and WIVS-FM T268A (B). (C) UV-Vis data for WIVS-FM/Fe-DPIX (purple) and native BM3h/heme (blue). See Table S3.2 for the exact peak wavelengths.

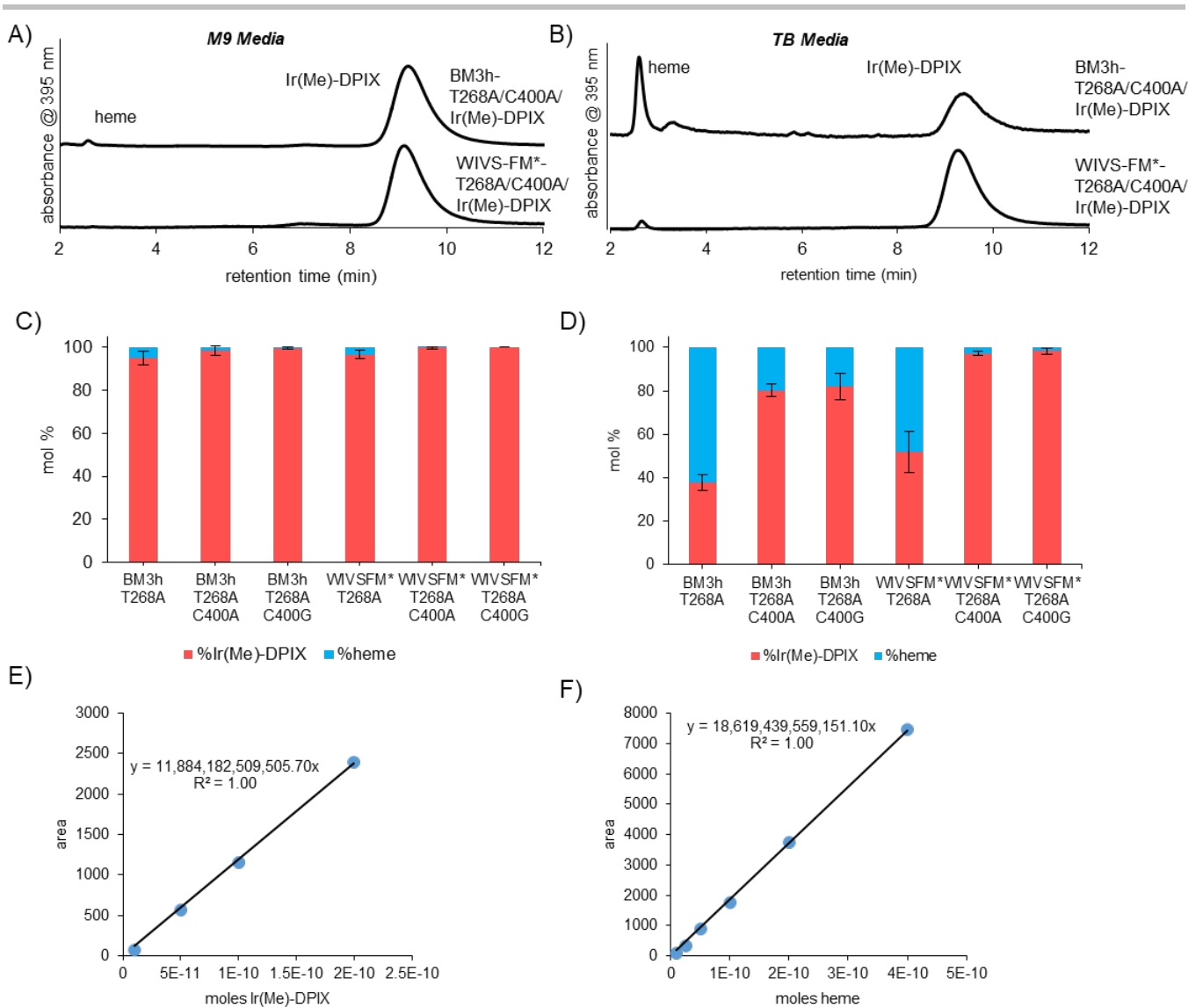


Figure S2. HPLC analysis of Ir(Me)-DPIX content in protein preparations.

Sample HPLC traces of BM3h-T268A/C400A and WIV-FM*-T268A/C400A from expressions supplemented with Ir(Me)-DPIX, in minimal media (A) and rich (TB) media (B). See **Figure 2** in main text for HPLC traces of other variants. Also shown are bar graphs representing mol % Ir(Me)-DPIX (red) and heme (blue) for each variant expressed in minimal media (C) and TB (D) as determined by HPLC analysis of purified proteins. Error bars represent standard deviations determined from n=3 independent experiments. E) HPLC calibration curves for Ir(Me)-DPIX and heme (F) used to calculate the concentration of these cofactors in proteins.

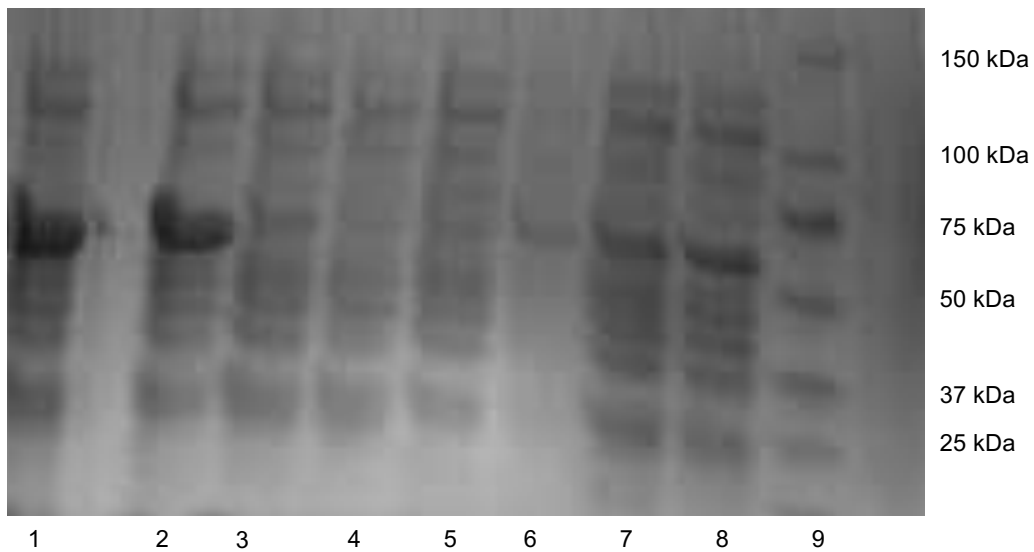


Figure S3. Relative yields of BM3h T268A, WIVS-FM T268A and WIVS-FM* T268A variants with Ir(Me)-DPIX.
SDS-PAGE analysis of cell lysate following expression of BM3h variants (~54 kD) in minimal media supplemented with Ir(Me)-DPIX. 1) BM3h T268A 2) BM3h T268A/C400A 3) WIVS-FM T268A 4) WIVS-FM T268A/C400A 5) WIVS-FM T268A/C400G 6) WIVS-FM* T268A 7) WIVS-FM* T268A/C400A 8) WIVS-FM* T268A/C400G 9) Ladder with the 70 kD and 50 kD markers labeled.

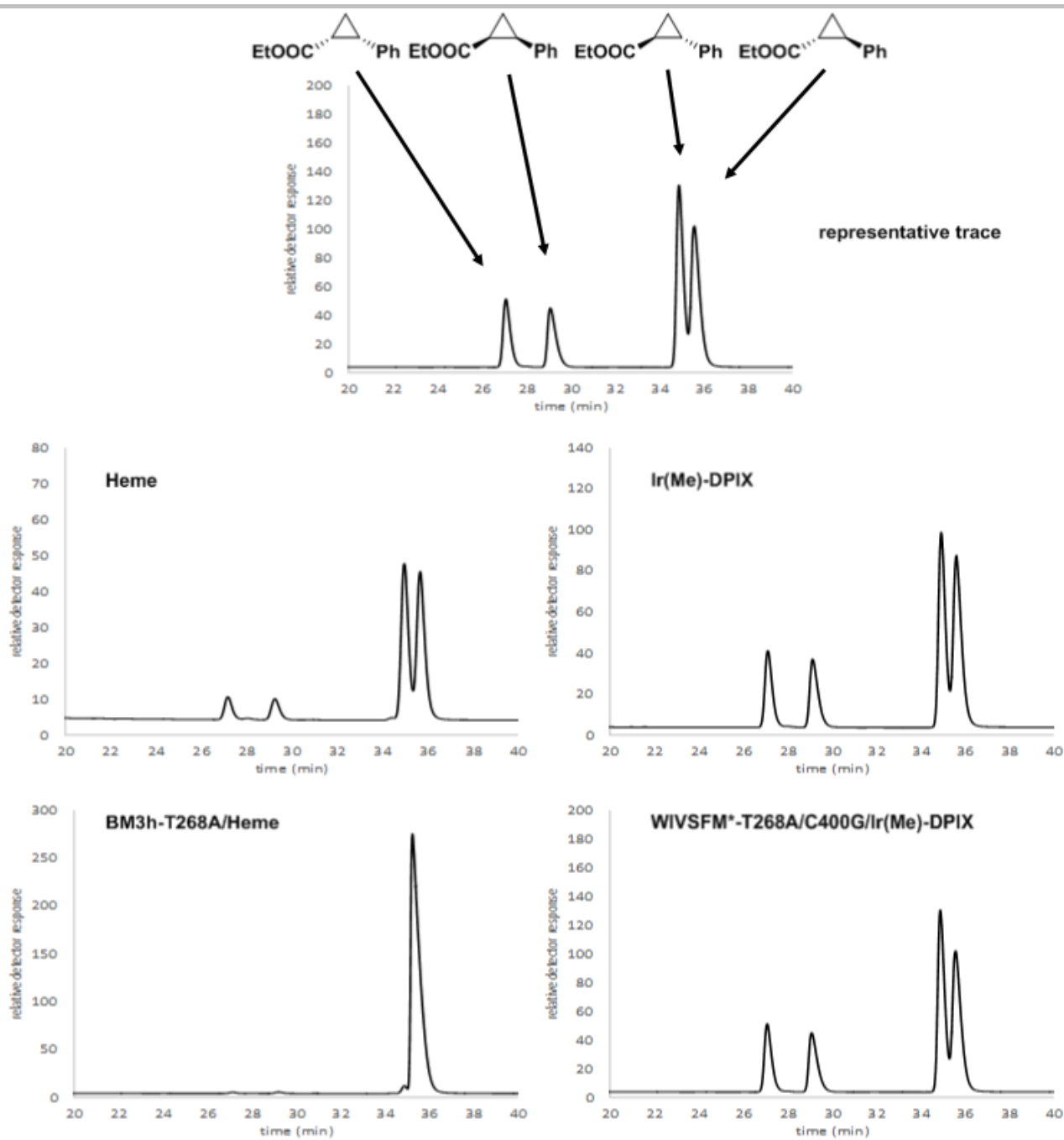


Figure S4. GC chromatographs for cyclopropanation reaction products using ethyl diazoacetate and styrene. The retention times and assignments for each enantiomer product are shown, determined previously (top).^[3]

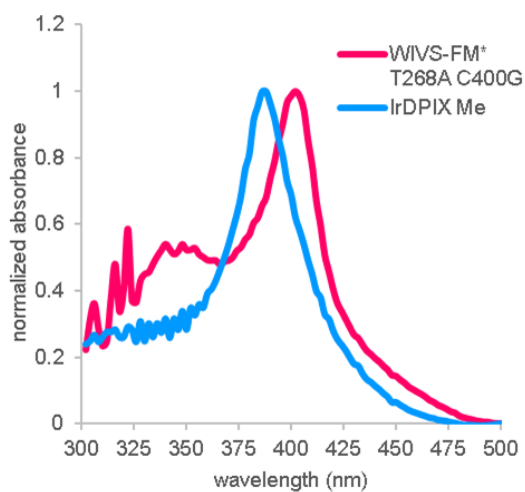
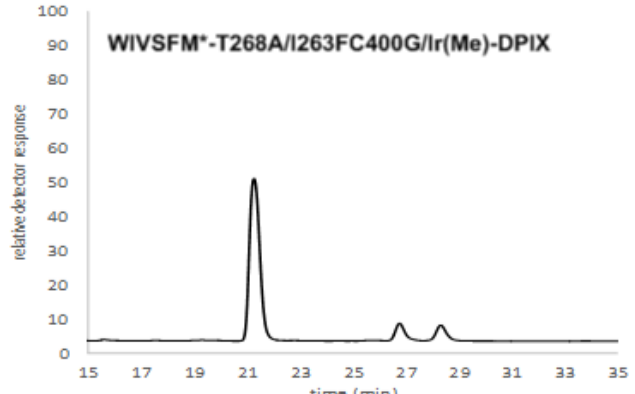
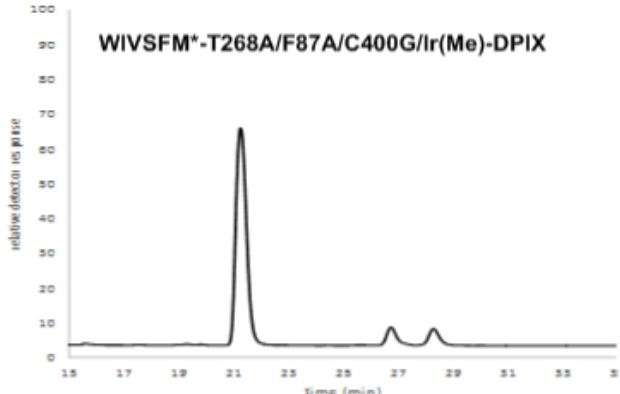
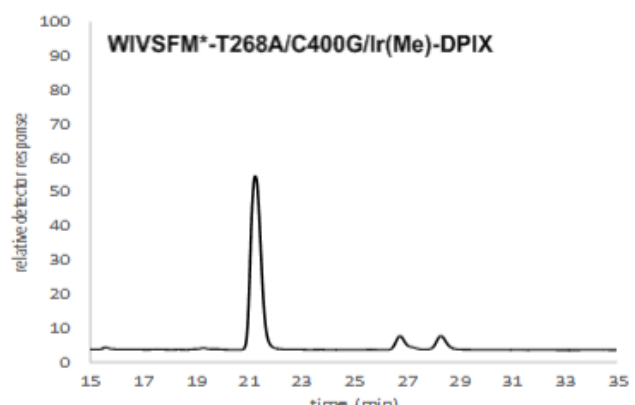
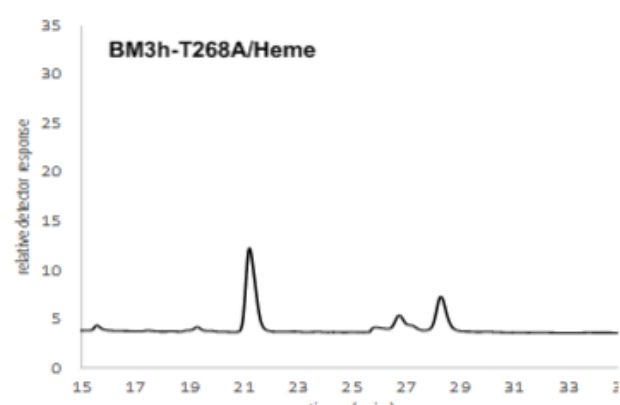
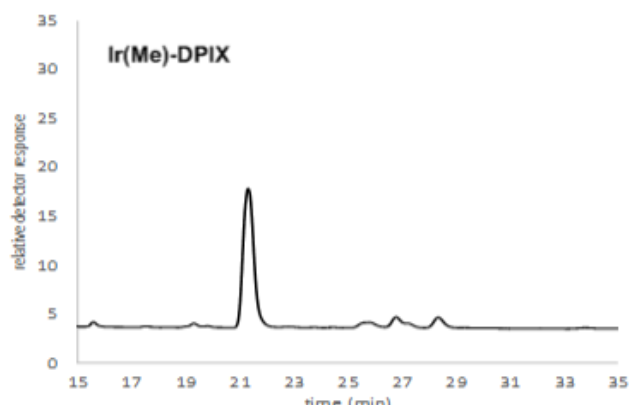
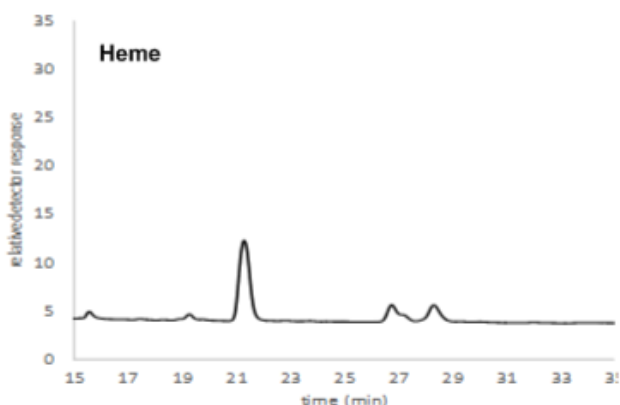
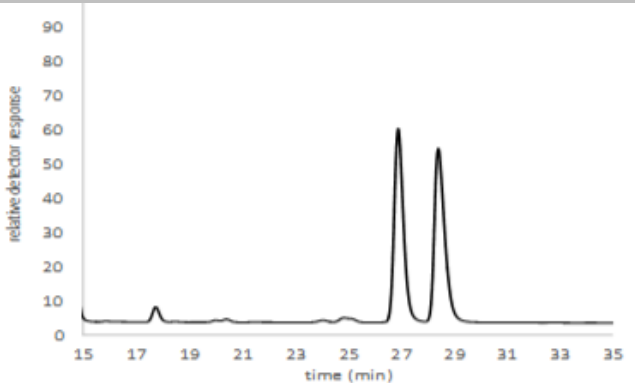
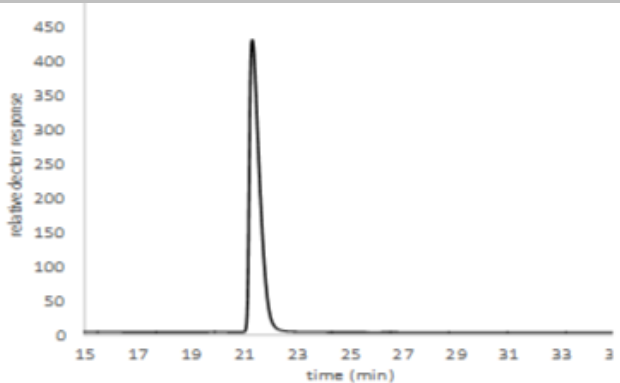


Figure S5. Absorbance shifts for WIVS-FM* bound and free IrDPIX Me are retained following an enzymatic reaction. UV-Vis data is shown for IrDPIX Me substituted WIVS-FM* T268A C400G and free IrDPIX Me following a 16 hour cyclopropanation reaction.



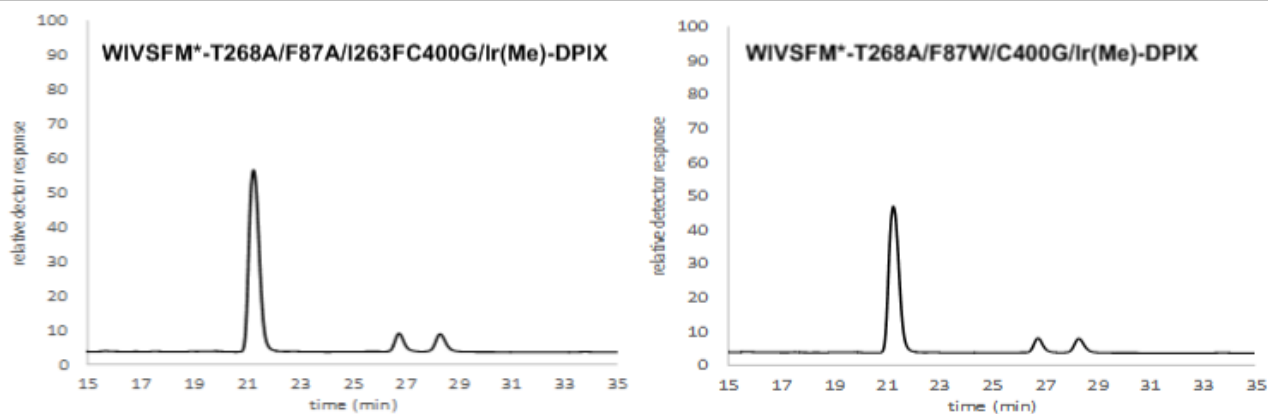
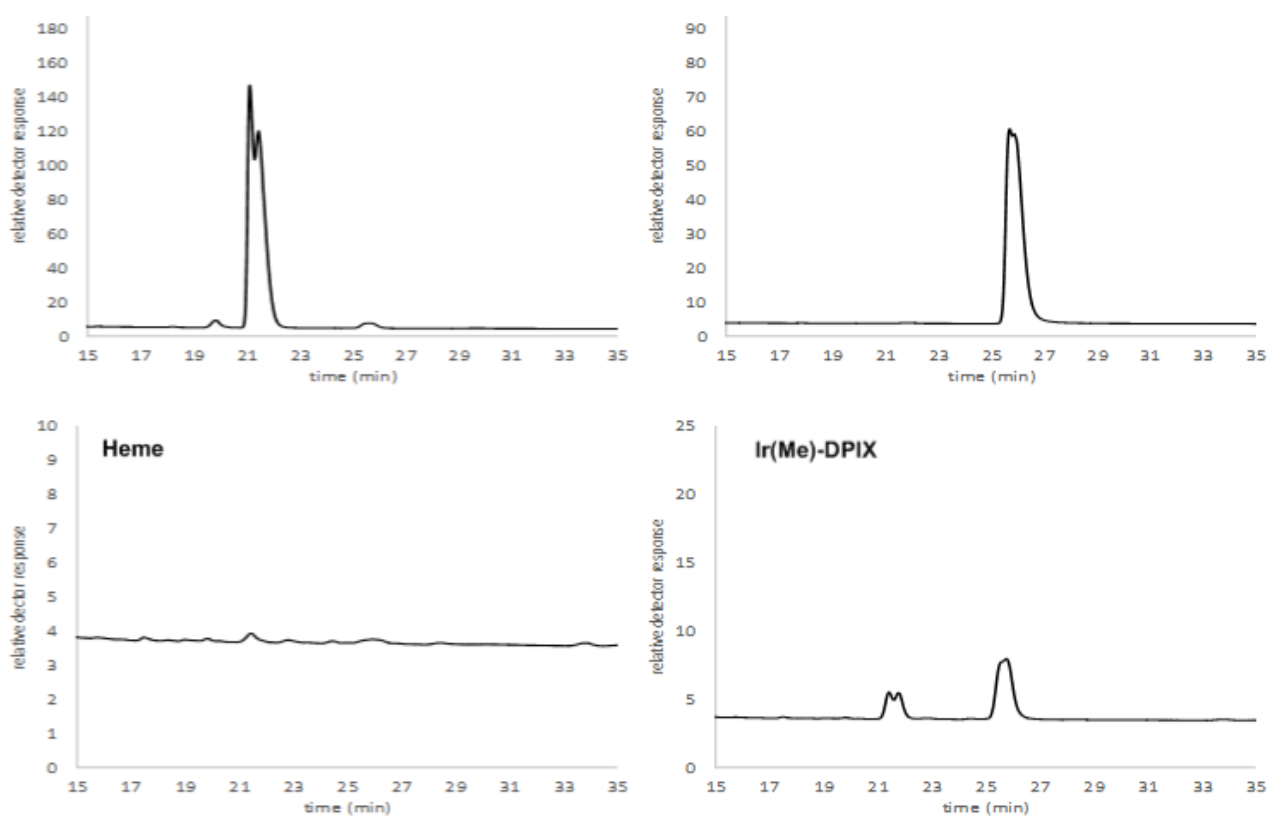


Figure S6. GC chromatographs for cyclopropanation products using ethyl diazoacetate and tert-butyl acrylate.

The retention times for the purified trans (top left) and cis (top right) enantiomer products. Relative detector responses for the WIVSFM*-T268A/C400G variants that were screened for improved cyclopropanation activity are also shown. Mutations at the F87 positions (including F87A) and I263F were chosen as they have been shown to have an effect on carbenoid and nitrenoid insertion activity of hemoproteins.^[9,10] Traces showing the separation of the trans enantiomers are shown in figure S8.



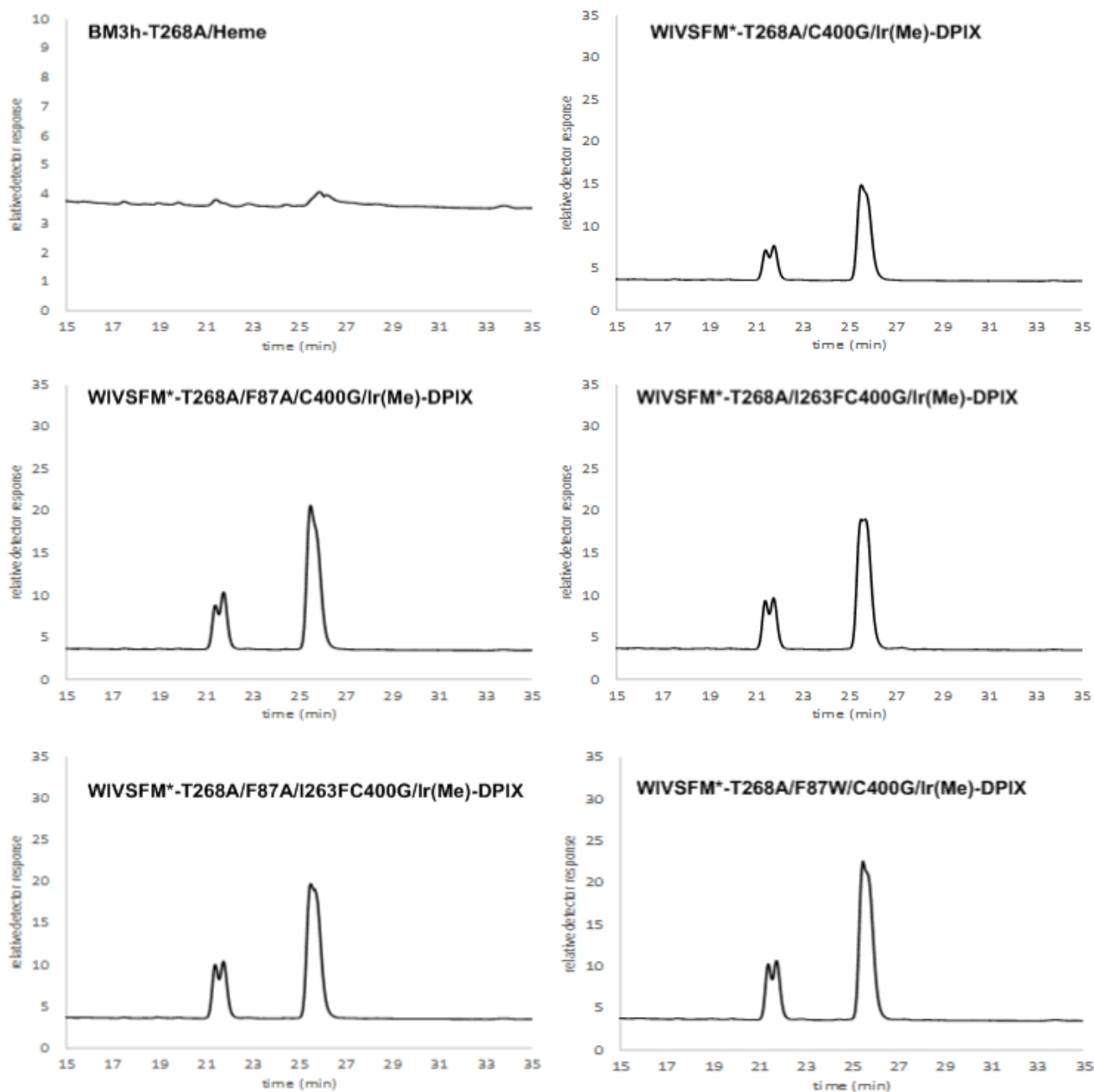


Figure S7. GC chromatographs for cyclopropanation products using ethyl diazoacetate and 1-octene.

The retention times for the purified trans (top right) and cis (top left) enantiomer products are shown. Relative detector responses for the WIVS-FM*-T268A/C400G variants that were screened for improved cyclopropanation activity are also shown. Mutations at the F87 positions (including F87A) and I263F were chosen as they have been shown to have an effect on carbenoid and nitrenoid insertion activity of hemoproteins.^[9,10] Traces showing the separation of the cis enantiomer products are shown in figure S9.

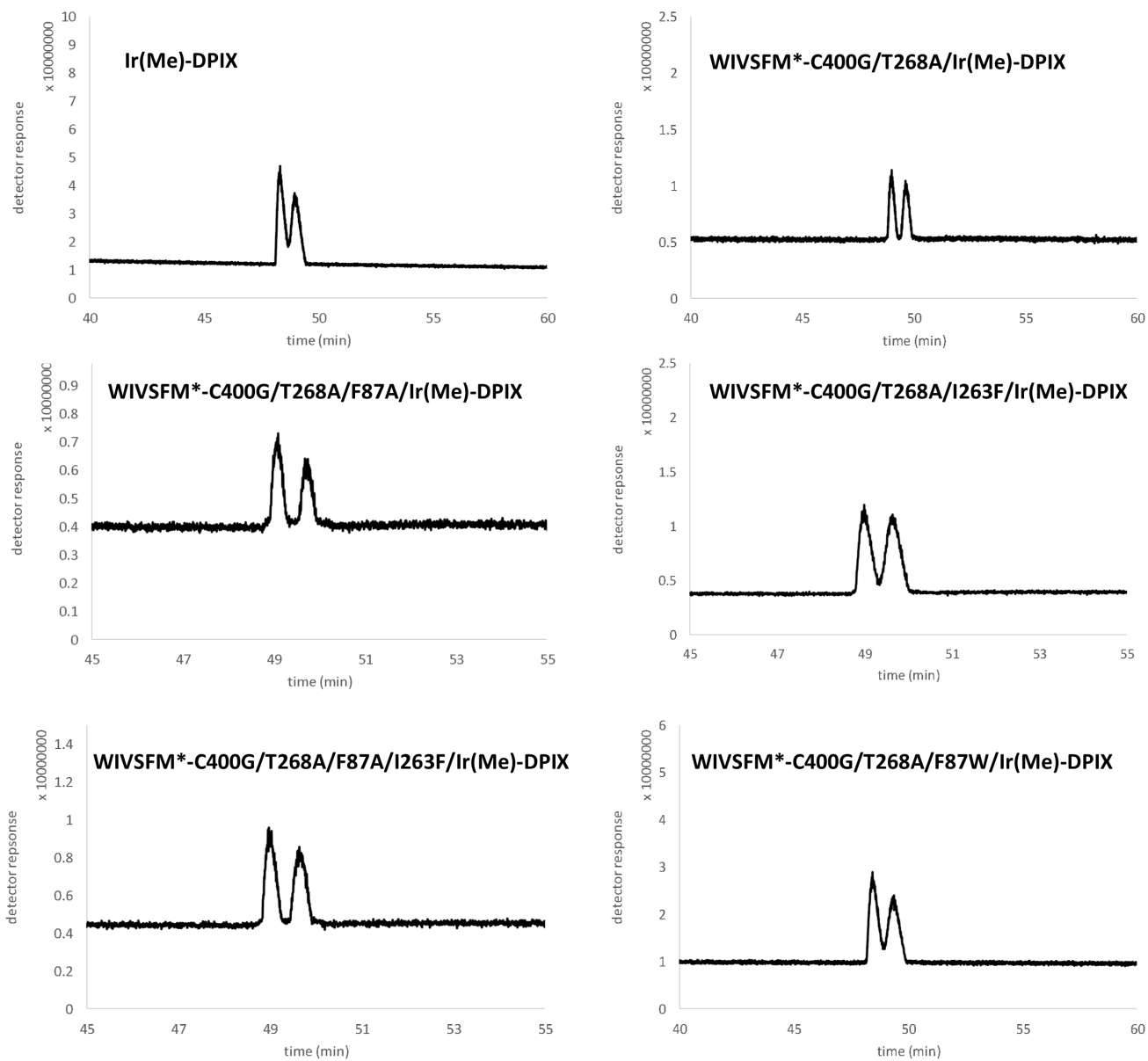


Figure S8. GC/MS chromatographs separating the *trans* cyclopropanation products using ethyl diazoacetate and tert-butyl acrylate.

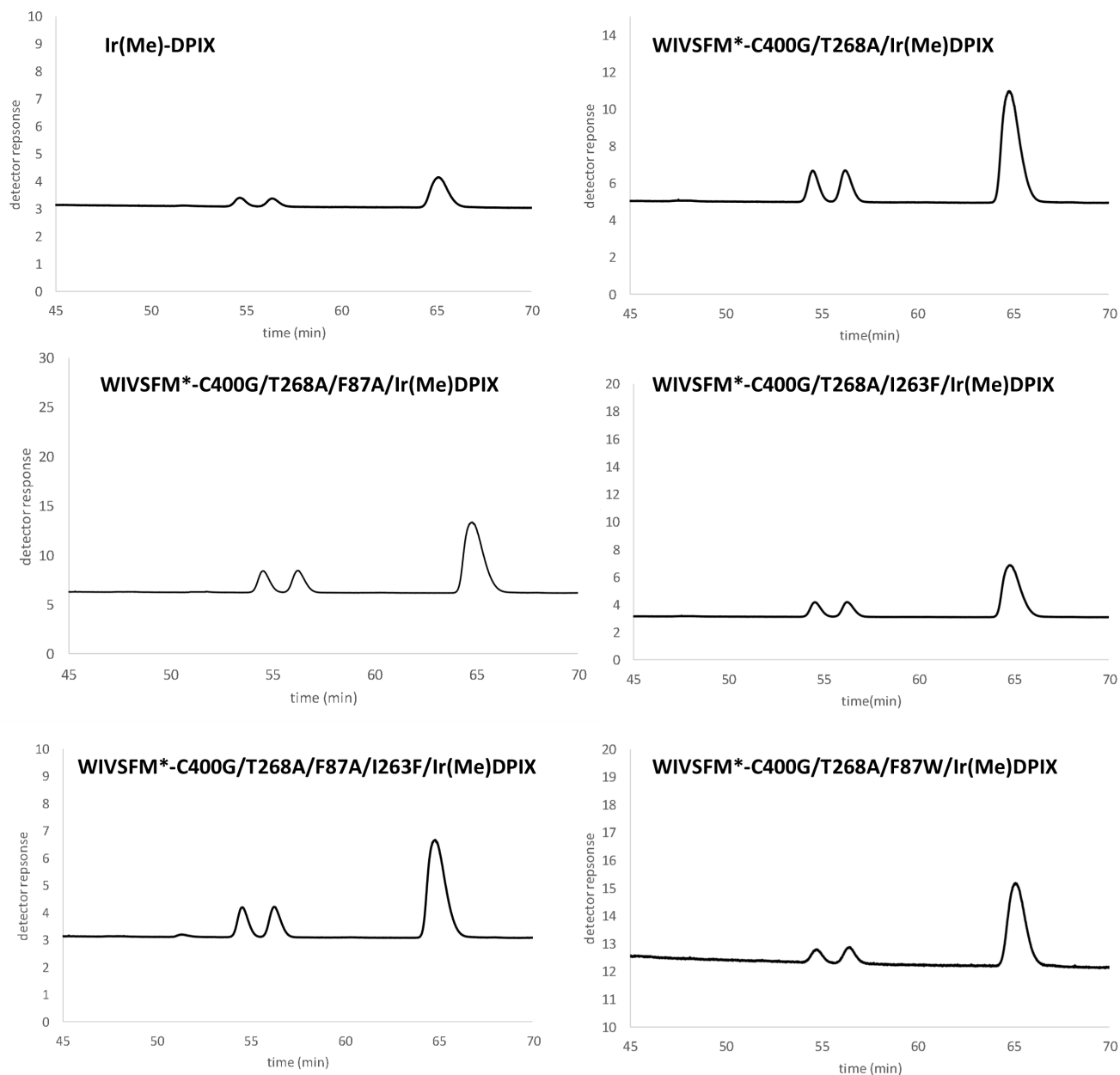


Figure S9. GC Chromatographs separating the *cis* cyclopropanation products using ethyl diazoacetate and 1-octene.

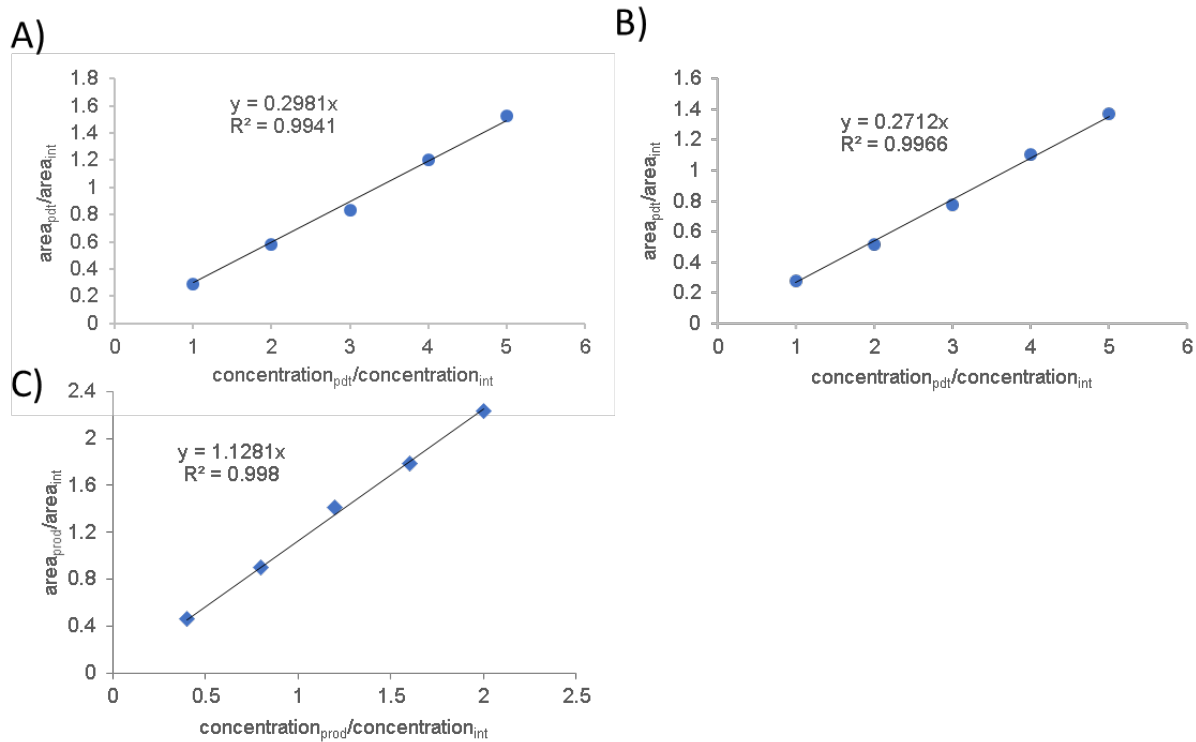
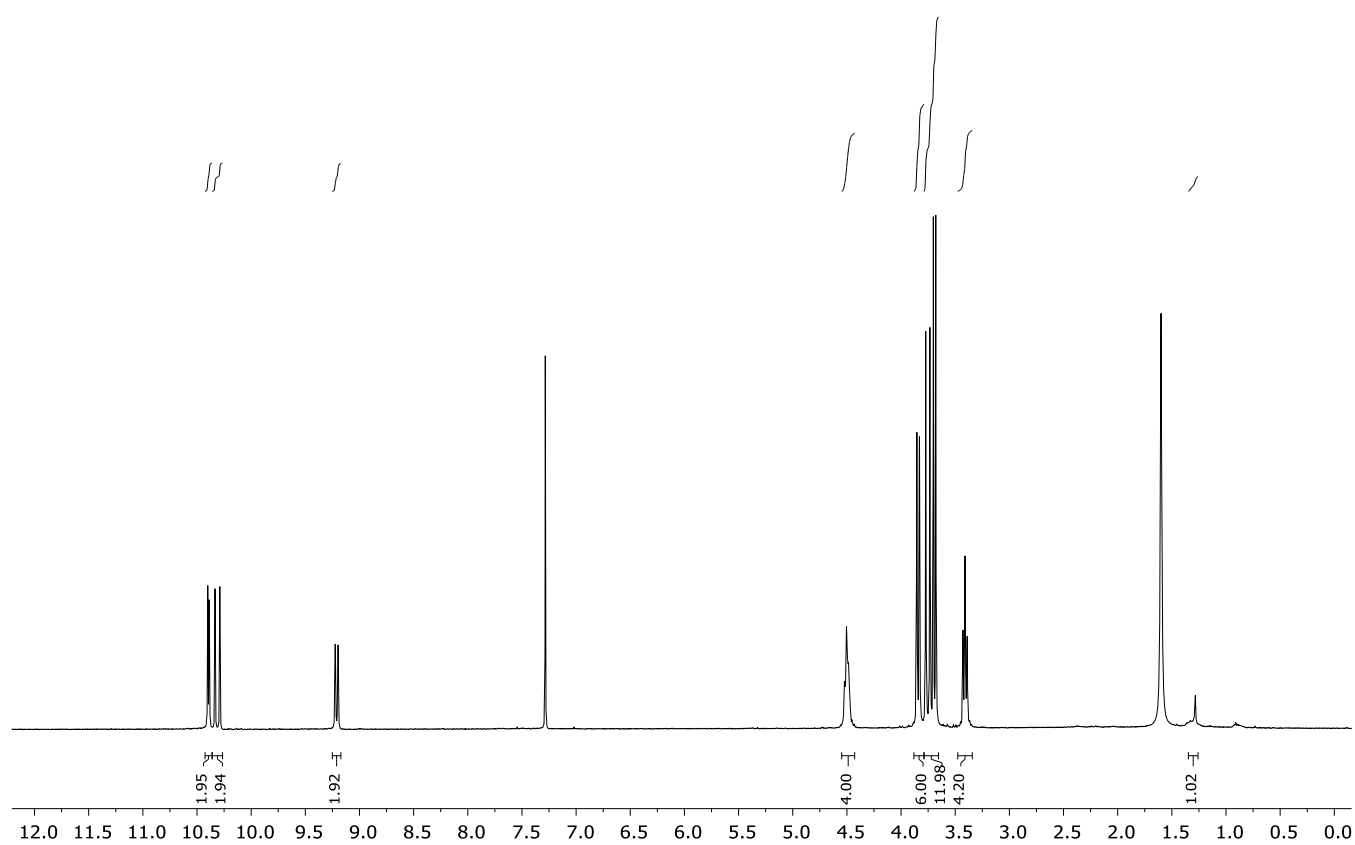
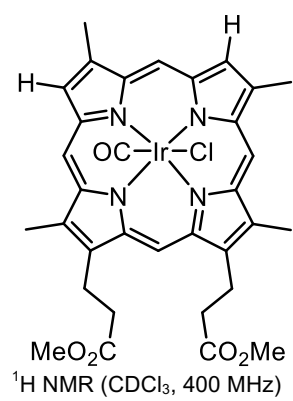
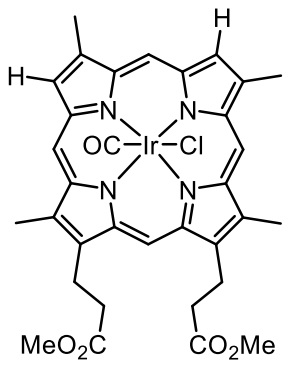


Figure S10. Calibration curves used to determine cyclopropane product concentrations.

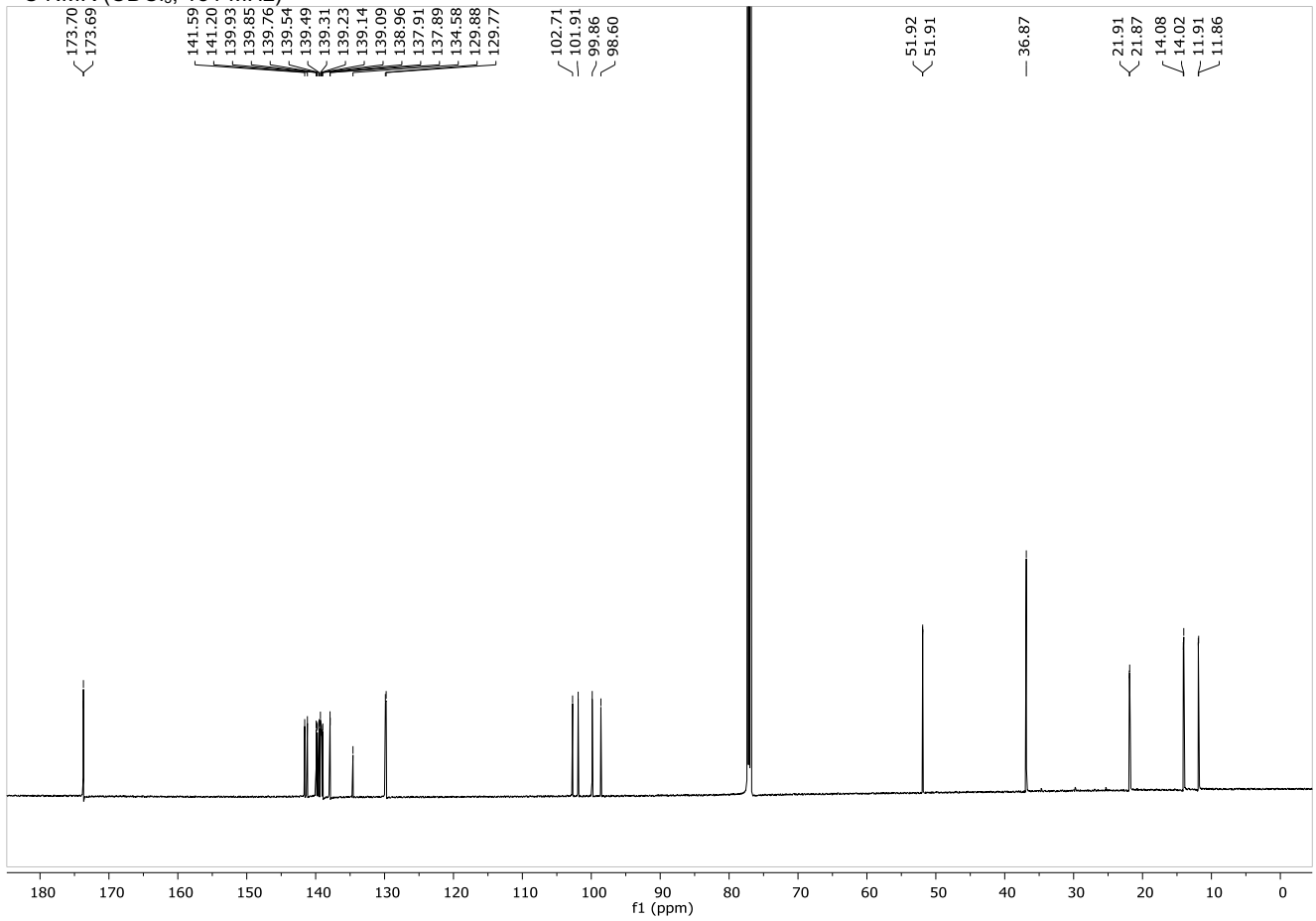
(A) Calibration curve for 1-(tert-butyl) 2-ethyl cyclopropane-1,2-dicarboxylate using 2mM propiophenone as an internal standard. (B) Calibration curve for ethyl 2-hexylcyclopropane-1-carboxylate using 2mM propiophenone as an internal standard. (C) Previously reported calibration curve for 2-phenylcyclopropane-1-carboxylate using cyclopropylphenyl ketone as an internal standard.^[8]

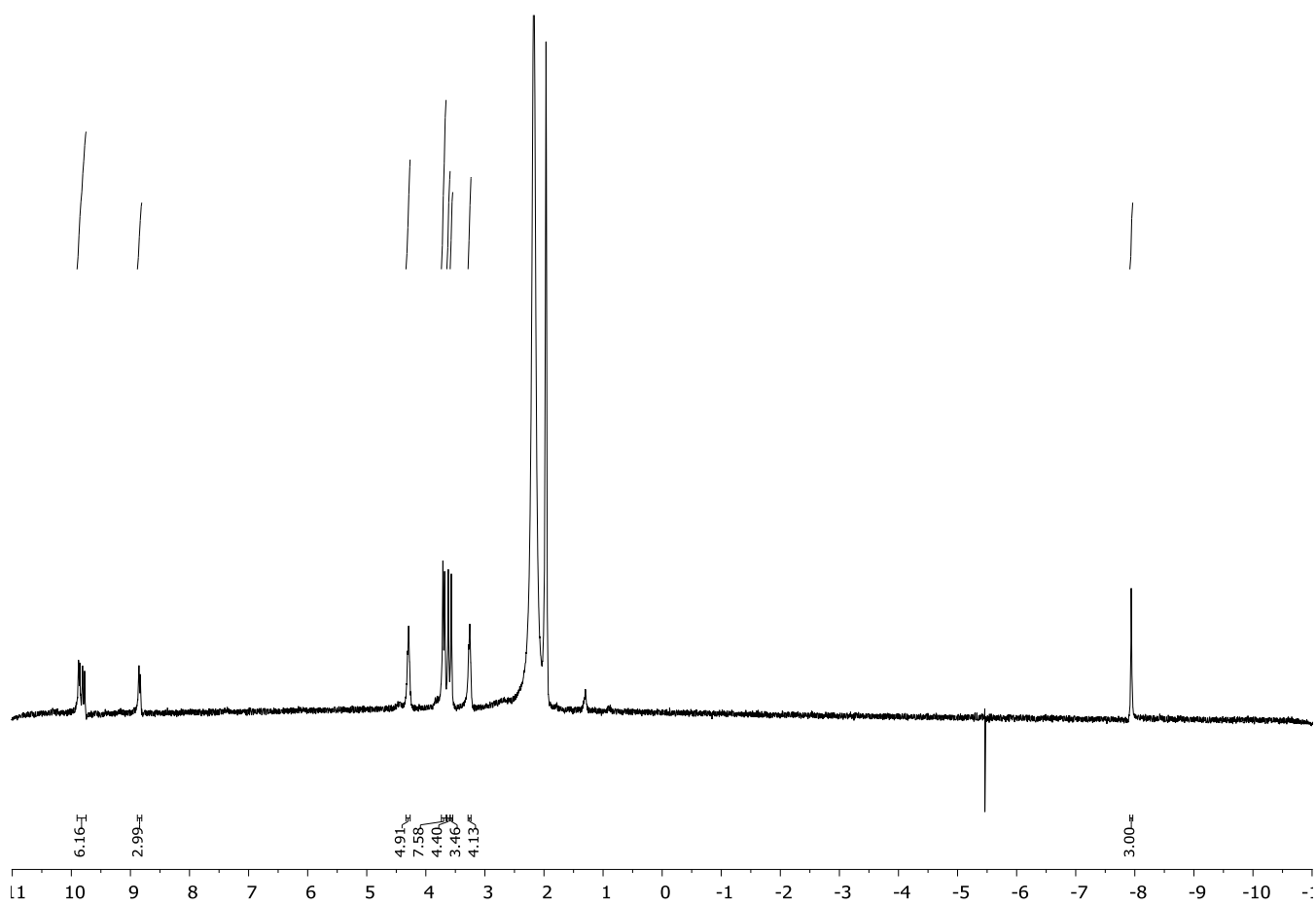
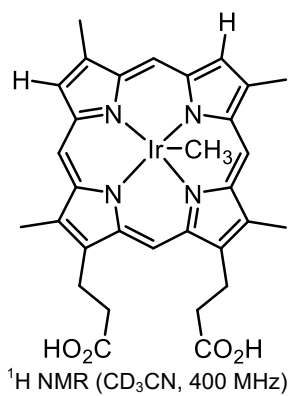
NMR data

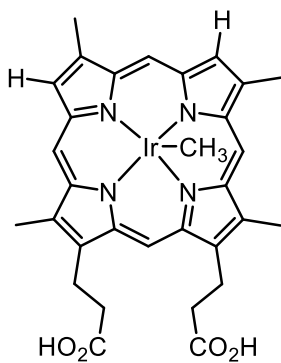




¹³C NMR (CDCl₃, 151 MHz)

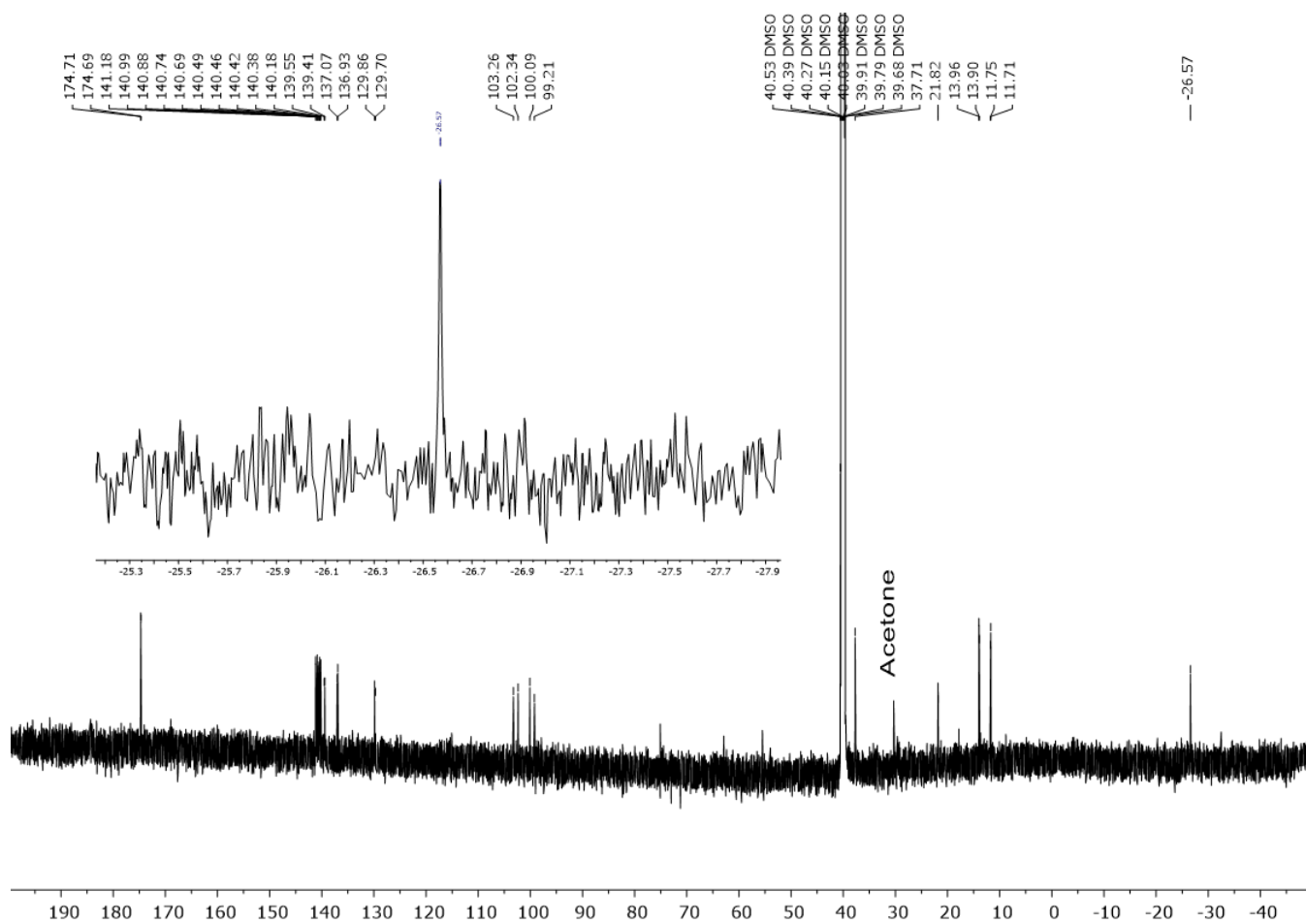






¹³C NMR (DMSO-d₆, 151 MHz)

Inset shows resonance corresponding to Ir-bound CH₃.



References

- [1] G. R. Fulmer, A. J. M. Miller, N. H. Sherden, H. E. Gottlieb, A. Nudelman, B. M. Stoltz, J. E. Bercaw, K. I. Goldberg, *Organometallics* **2010**, *29*, 2176–2179.
- [2] H. M. Key, P. Dydio, D. S. Clark, J. F. Hartwig, *Nature* **2016**, *534*, 534–537.
- [3] J. G. Gober, A. E. Rydeen, E. J. Gibson-O'Grady, J. B. Leuthaeuser, J. S. Fetrow, E. M. Brustad, *ChemBioChem* **2015**, *17*, 394–397.
- [4] Y. Chen, J. V Ruppel, X. P. Zhang, *J. Am. Chem. Soc.* **2007**, *129*, 12074–5.
- [5] P. Kumar, A. Dubey, A. Harbindu, K. Faber, U. P. Dhokte, C. W. Doecke, L. M. H. Zollars, E. D. Moher, V. V. Khau, B. Kosmrlj, et al., *Org. Biomol. Chem.* **2012**, *10*, 6987–6994.
- [6] E. M. Brustad, V. S. Lelyveld, C. D. Snow, N. Crook, S. T. Jung, F. M. Martinez, T. J. Scholl, A. Jasanoff, F. H. Arnold, *J. Mol. Biol.* **2012**, *422*, 245–262.
- [7] V. S. Lelyveld, E. Brustad, F. H. Arnold, A. Jasanoff, *J. Am. Chem. Soc.* **2011**, *133*, 649–651.
- [8] E. W. Reynolds, M. W. McHenry, F. Cannac, J. G. Gober, C. D. Snow, E. M. Brustad, *J. Am. Chem. Soc.* **2016**, *138*, 12451–12458.
- [9] P. S. Coelho, E. M. Brustad, A. Kannan, F. H. Arnold, *Science* **2013**, *339*, 307–10.
- [10] C. C. Farwell, R. K. Zhang, J. a. McIntosh, T. K. Hyster, F. H. Arnold, *ACS Cent. Sci.* **2015**, *1*, 89–93.

Author Contributions

EWR, TDS, and EMB conceived and designed experiments. EWR, TDS, MWM, JWW carried out experiments. EWR, TDS, and EMB wrote the manuscript.